XL CILAMCE
IBERO-LATIN AMERICAN CONGRESS ON COMPUTATIONAL METHODS IN ENGINEERING
NOVEMBER 11-14, 2019
Praiamar Natal Hotel & Convention Natal, RN-BRAZIL

EVALUATION OF A HOMOGENIZATION-BASED APPROACH FOR ANALYSIS OF METAL MATRIX COMPOSITES BY THE BOUNDARY ELEMENT METHOD CONSIDERING PHASE DEBONDING

Gabriela R. Fernandes
José J. C. Pituba
gabrielar.fernandes@gmail.com
julio_pituba@ufg.br
Laboratory of Computational Modelling, Civil Engineering Department, Federal University of Goiás, Av Dr. Lamartine Pinto de Avelar, 1120, Setor Universitário- CEP 75700-000 Catalão – GO Brazil.

Abstract. A formulation of the Boundary Element Method (BEM) to perform analysis of ductile heterogeneous microstructures considering phase debonding is presented in the context of multi-scale analysis. The microstructure is modelled by a zoned plate, where different mechanical behaviour can be adopted for each sub-region. To solve the domain integrals written in terms of in-plane displacements or plastic forces, the matrix and inclusions domains have to be discretized into cells where the displacements and forces are approximated. In multi-scale analysis, a point of the macrocontinuum is represented by a Representative Volume Element (RVE) which in this work, to model metal matrix composites, is assumed to contain a ductile matrix, rigid inclusions and interface zone. The rigid inclusions are considered as elastic medium whereas the matrix behaviour is governed by the Von Mises elastoplastic model with linear strain hardening. The phase debonding is modelled by a cohesive fracture model using embedded cohesive contact finite elements in the boundary element mesh. The homogenized results are compared with the ones obtained from a model based on Finite Element Method (FEM). The accuracy of the results show the capability of the new formulation based on BEM to deal with complex microstructures.

Keywords: Boundary elements, Homogenization, Metal matrix composites, Cohesive zone model.

1 Introduction

The boundary element method (BEM) has already proved to be a suitable numerical tool to deal with plate problems. The method is particularly recommended to evaluate internal force concentrations due to loads distributed over small regions that very often appear in practical problems. Several works have already considered BEM formulations to treat different kinds of problems as can be seen in the works Aliabadi [1], Beskos [2], Brebbia, Telles and Wrobel [3], Fernandes and de Souza Neto [4], Fernandes and Rosa Neto [5].

In general, the materials, even the metallic, are heterogeneous at the micro and grain scales. Besides, the material microstructure can be also appropriately manipulated by adding certain constituents to a matrix phase, in order to change the material properties to attend specific applications, as the MMCs (metal matrix composites). As any heterogeneity of the material as well as the microcracking initiation and propagation in the micro-scale affect directly the macro-continuum response, therefore modeling heterogeneous material in different scales is very important to better represent the behavior of such complex materials as discussed in Gal and Kryvoruk [6]; Nguyen, Lloberas, Stroeven and Sluys [7]; Pituba, Fernandes and de Souza Neto [8].

In multi-scale analysis, the RVE (representative volume element) represents the microstructure, at grain level, of the macro-continuum at the infinitesimal material neighborhood of a point as can be seen in the works de Souza Neto and Feijóo [9]; Fernandes, Pituba and de Souza Neto ([10], [11]).

In this paper a BEM formulation to perform analysis of ductile heterogeneous microstructures considering phase debonding, in the context of multi-scale analysis, is presented. The RVE is considered as a zoned plate, whose sub-regions define its different materials. Besides, at interfaces cohesive contact finite elements have been defined, whose behaviour are governed by a cohesive fracture model, in order to represent the phase debonding that occur during the fracture process. The presented formulation is developed in details in Fernandes and Pituba [12].

2 Basic Equations

The domain Ω of a heterogeneous microstructure is assumed to consist in general of a solid part, Ω^s and a void part Ω^v, being $\Omega = \Omega^v \cup \Omega^s$, where the solid part can be made of distinct materials (or phases), each one defined by a sub-domain, whose material can have different elastics properties. Without loss of generality, let us consider the microstructure depicted in Fig. 1 represented by a zoned plate, where sub-region Ω_1 represents the matrix whose external boundary is Γ_1, sub-region Ω_2 is an inclusion and Ω_3 a void. Besides, in Fig. 1 Γ_{jk} represents the interface between the adjacent sub-regions Ω_j and Ω_k and the Cartesian system of co-ordinates (axes x_1 and x_2) is defined on the plate surface.

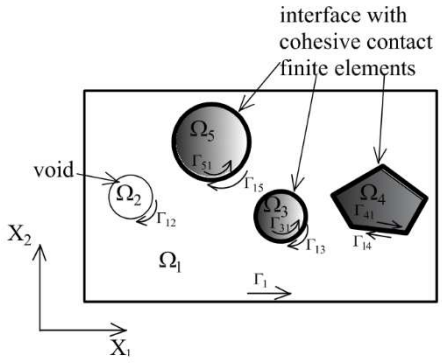

Figure 1- Heterogeneous microstructure represented by a zoned plate with superposed cohesive contact elements on the interfaces

Along the interface Γ_{jk} the phase debonding phenomenon will be modelled by contact and cohesive fracture models which will govern the mechanical behaviour in the additional cohesive contact finite elements defined on the interfaces (see Fig. 1). For a point placed at any of those sub-regions, the in-plane equilibrium equation can be defined:

$$\dot{N}_{ij},_j + \dot{\bar{b}}_i = 0 \qquad \text{i, j=1, 2} \tag{1}$$

where $\dot{\bar{b}}_i = \dot{b}_i t$, b_i are body forces distributed over the plate middle surface and N_{ij} is the membrane internal force. As this work only deals with small strain problems the total strain will be split into its elastic and plastic parts, $\dot{\varepsilon}_{ij}^e$ and $\dot{\varepsilon}_{ij}^p$ respectively, as follows:

$$\dot{\varepsilon}_{ij} = \dot{\varepsilon}_{ij}^e + \dot{\varepsilon}_{ij}^p \qquad \text{i, j= 1, 2} \tag{2}$$

Note that when the phase debonding is taken into account, the total strain $\dot{\varepsilon}_{ij}$ is divided into two parts: the continuum strain $\dot{\bar{\varepsilon}}_{ij}$ and the strain due to the phase debonding $\dot{\varepsilon}_{ij}^{cf}$ i.e.: $\dot{\varepsilon}_{ij} = \dot{\bar{\varepsilon}}_{ij} + \dot{\varepsilon}_{ij}^{cf}$. By applying the Hooke's law the stress tensor rate $\dot{\sigma}_{ij}$ (computed according to the constitutive model), as well as the force $\dot{N}_{ij}$, can be related to the elastic part $\dot{\varepsilon}_{ij}^{e}$ of the strain tensor rate and the membrane force predictor $\dot{N}_{ij}^t$ (often defined as elastic trial used in non-linear algorithms) related to the total strain $\dot{\varepsilon}_{ij}$. Thus, the forces $\dot{N}_{ij}^t$, for plane stress conditions, can be written in terms of the in-plane deformations ε_{ij} as follows:

$$\dot{N}_{ij}^t = \frac{\overline{E}}{\left(1-\nu^2\right)}\left[\nu\ \dot{\varepsilon}_{kk}\delta_{ij} + \left(1-\nu\ \right)\dot{\varepsilon}_{ij}\right] \tag{3a}$$

or

$$\dot{N}_{ij}^t = \frac{\overline{E}}{\left(1-\nu^2\right)}\left[\nu\ \dot{\bar{\varepsilon}}_{kk}\delta_{ij} + \left(1-\nu\ \right)\dot{\bar{\varepsilon}}_{ij}\right] + \frac{\overline{E}}{\left(1-\nu^2\right)}\left[\nu\ \dot{\varepsilon}_{kk}^{cf}\delta_{ij} + \left(1-\nu\ \right)\dot{\varepsilon}_{ij}^{cf}\right] = \dot{\bar{N}}_{ij} + \dot{N}_{ij}^{cf} \tag{3b}$$

where $\dot{\bar{N}}_{ij}$ are the forces related to the continuous strains while $\dot{N}_{ij}^{cf}$ is related to the phase debonding phenomenon, $\overline{E} = Et$, E is the Young's modulus, ν the Poisson's ratio, t the plate thickness and δ_{ij} the Kronecker delta. Therefore, the membrane force rate $\dot{\bar{N}}_{ij}$ can be written as:

$$\dot{\bar{N}}_{ij} = \dot{N}_{ij} + \dot{N}_{ij}^P - \dot{N}_{ij}^{cf} = \dot{N}_{ij} + \dot{N}_{ij}^0 \tag{4}$$

Observe that when an elastoplastic model is considered to govern the material behavior and cohesive contact finite elements are considered at interfaces, the inelastic forces $\dot{N}_{ij}^0$ can have contributions of these two different dissipative phenomena, i.e.: $\dot{N}_{ij}^0 = \dot{N}_{ij}^p - \dot{N}_{ij}^{cf}$. On the other hand, the plastic forces are given by: $\dot{N}_{ij}^p = \dot{N}_{ij}^t - \dot{N}_{ij}$, where the trial membrane forces $\dot{N}_{ij}^t$ are computed considering the total strain (see equation 3). The inelastic forces related to the contact fracture model, adopted to govern the material behavior in the finite elements defined on the interfaces, is given by: $\dot{N}_{ij}^{cf} = \dot{N}_{ij}^t - \dot{\bar{N}}_{ij}$. The forces $\dot{\bar{N}}_{ij}$ related to the continuous strains (see Eq. 3b), in the present paper, corresponds to the membrane forces computed before solving the RVE iterative procedure necessary to achieve its equilibrium (see more details further), which is solved in terms of displacement

fluctuations (or strain fluctuations). Note that after solving the RVE equilibrium problem, if the phase debonding takes place the displacement field will no longer be continuous on the interfaces and the total strains will have the part $\dot{\varepsilon}_{ij}^{cf}$ related to this discontinuity. The problem definition is then completed by assuming the following boundary conditions over Γ: $U_i = \overline{U}_i$ on Γ_u (in-plane displacements) and $P_i = \overline{P}_i$ on Γ_p (in-plane tractions), where $\Gamma_u \cup \Gamma_p = \Gamma$.

3 Integral Representation For Displacement

Writing the fundamental strains ε_{kij}^{m*} of sub-region Ω_m in terms of the values ε_{kij}^{*} and the fundamental membrane force N_{kij}^{m*} in terms of ν and N_{kij}^{*}, being ε_{kij}^{*}, $\overline{E}$, ν and N_{kij}^{*} referred to the sub-region where the load point *s* is placed, from Betti's Theorem, considering eq.(4), the following equation can be obtained for any sub-region Ω_m (see more details in Fernandes and Pituba [12]):

$$\int_{\Omega} \varepsilon_{kij}^{*} \overline{N}_{ij} d\Omega = \sum_{m=1}^{N_S} \left[\frac{\overline{\overline{E}}_m}{\overline{\overline{E}}} \frac{\nu_m}{\nu} \int_{\Omega_m} \varepsilon_{ij} N_{kij}^{*} d\Omega + \overline{\overline{E}}_m \left(1 - \frac{\nu_m}{\nu}\right) \int_{\Omega_m} \varepsilon_{ij} \varepsilon_{kij}^{*} d\Omega_m \right] - \int_{\Omega_m} \varepsilon_{kij}^{*} N_{ij}^{0(m)} d\Omega \quad \text{i, j, k=1, 2} \quad (5)$$

where N_s is the sub-regions number; $\overline{\overline{E}}_m = \dfrac{\overline{E}_m}{\left(1-\nu_m^{\,2}\right)}$.

Integrating eq. (5) by parts we obtain the following representation of in-plane displacements:

$$C_{k1}\dot{u}_1(s) + C_{k2}\dot{u}_2(s) = -\frac{\overline{\overline{E}}_1 \nu_1}{\overline{\overline{E}}\nu} \int_{\Gamma_1} \left(\dot{u}_1(P) p_{k1}^{*}(s,P) + \dot{u}_2(P) p_{k2}^{*}(s,P)\right) d\Gamma +$$

$$- \sum_{m=1}^{N_{inc}} \frac{\left(\overline{\overline{E}}_m \nu_m - \overline{\overline{E}}_1 \nu_1\right)}{\overline{\overline{E}}\nu} \int_{\Gamma_{m1}} \left(\dot{u}_1(P) p_{k1}^{*}(s,P) + \dot{u}_2(P) p_{k2}^{*}(s,P)\right) d\Gamma_{m1}$$

$$- \sum_{m=1}^{N_{voids}} \frac{\overline{\overline{E}}_1 \nu_1}{\overline{\overline{E}}\nu} \int_{\Gamma_{1m}} \left(\dot{u}_1(P) p_{k1}^{*}(s,P) + \dot{u}_2(P) p_{k2}^{*}(s,P)\right) d\Gamma_{1m} + \int_{\Gamma_1} \left(u_{k1}^{*}(s,P)\dot{p}_1(P) + u_{k2}^{*}(s,P)\dot{p}_2(P)\right) d\Gamma +$$

$$- \overline{\overline{E}}_1 \left(1 - \frac{\nu_1}{\nu}\right) \int_{\Gamma_1} \left[\dot{u}_1(P)\varepsilon_{k1}^{*}(s,P) + \dot{u}_2(P)\varepsilon_{k2}^{*}(s,P)\right] d\Gamma + \sum_{m=1}^{N_s} \overline{\overline{E}}_m \left(1 - \frac{\nu_m}{\nu}\right) \int_{\Omega_m} \dot{u}_i(p)\varepsilon_{kij,j}^{*}(s,p) d\Omega_m$$

$$- \sum_{m=1}^{N_{inc}} \left[\overline{\overline{E}}_m \left(1 - \frac{\nu_m}{\nu}\right) - \overline{\overline{E}}_1 \left(1 - \frac{\nu_1}{\nu}\right) \right] \int_{\Gamma_{m1}} \left[\dot{u}_1(P)\varepsilon_{k1}^{*}(s,P) + \dot{u}_2(P)\varepsilon_{k2}^{*}(s,P)\right] d\Gamma_{m1} + \int_{\Omega_m} \varepsilon_{kij}^{*} \dot{N}_{ij}^{0(m)} d\Omega \quad \text{k, i, j=1,2} \quad (6)$$

where *k* is the fundamental load direction, N_{int} is the interfaces number; N_{voids} is the voids number; Ω_1 represents the matrix domain and Γ_1 its external boundary; Γ_{m1} represents an interface between the matrix and inclusion *m* and Γ_{1m} the interface between the matrix and a void *m;* the free terms values C_{k1} and C_{k2} depend on the position of the collocation point *s*.

4 Algebraic Equations

The integral representation Eq. (6) is transformed into algebraic expression after discretizing the external boundary and interfaces into elements and the domain into cells. Geometrically linear elements have been adopted, where linear shape functions have been assumed to approximate the variables. Moreover, triangular cells have been used to discretize the sub-regions domain, where the

displacements u_1 and u_2 are approximated by continuous linear shape functions, being their cell nodal values new independent values. Besides, the inelastic forces are assumed to be constant over the cell domain. Writing two displacements equations at boundary, interface and internal nodes, one can get the following set of equations where all values are written in terms of their increments (see more details in Fernandes and Pituba [12] and Fernandes, Crozariol, Furtado and Santos [13]):

$$\begin{bmatrix} [H]_{BB} & [H]_{Bi} \\ [H]_{iB} & [H]_{ii} \end{bmatrix} \begin{Bmatrix} \{\Delta U\}_B \\ \{\Delta U\}_i \end{Bmatrix} = \begin{bmatrix} [G]_{BB} \\ [G]_{iB} \end{bmatrix} \{\Delta P\}_B + [E] \{\Delta N^0\} \tag{7}$$

In Eq. (7) the subscript *B* is related to the external boundary while *i* is referred to interface and internal nodes; $\{\Delta N^0\}$, $\{\Delta U\}$ and $\{\Delta P\}$ are plastic forces, displacement and traction incremental vectors, respectively.

In a multi-scale analysis, the macro-strain has to be imposed to the RVE, leading to prescribe linear displacements over the external boundary as boundary conditions. Thus, in this case the unknowns vector {ΔX} computed from Eq. (7) are given by the in-plane tractions along the boundary and displacements at internal nodes. Besides, to solve the RVE equilibrium problem we also need to write the elastic forces $\dot{N}_{ij}^t$ equations at the center of all cells.

5 Homogenized values for Stress and Constitutive tensor

In the RVE the microscopic displacement field u_μ is split into the following sum:

$$u_\mu(y) = u_\mu^\varepsilon(y) + \tilde{u}_\mu(y) \tag{8}$$

where $u_\mu^\varepsilon(y)$ represents the displacement field obtained from the imposed macroscopic strain $\varepsilon(x)$, y represents an arbitrary point of the RVE; $\tilde{u}_\mu$ is the displacement fluctuation which represents the strain variation in the RVE.

On the other hand, to compute the constitutive response related to the material represented by the RVE, it is assumed sufficiently large in order to be considered as a continuum and the concept of stress to be valid at the microscopic scale. Then, it is also assumed that the strain tensor ε and the stress tensor σ at a point x of the macro-continuum are the volume average of their respective microscopic field (ε_μ or σ_μ) over the RVE associated with x (see details in de Souza Neto and Feijóo [9]; Fernandes, Pituba and de Souza Neto ([10], [11]); Fernandes and Pituba [12] and Fernandes, Crozariol, Furtado and Santos [13]). Besides, the homogenized constitutive tangent modulus C_{ep} can be also evaluated by applying the homogenization process.

After discretising the RVE into cells and elements (or finite elements for the FEM formulation developed in the works Souza Neto and Feijóo [9]; Fernandes, Pituba and de Souza Neto ([10], [11])), the following microscopic equilibrium equation must hold for a discretization *h*:

$$R_h = \int_{\Omega_\mu^h} f_y\left(\boldsymbol{\varepsilon} + B\tilde{u}_\mu\right) dV = 0 \tag{9}$$

where f_y is the constitutive functional defined by the adopted criterion, Ω_μ^h denotes the discretised RVE domain, N_{cel} is the number of cells used to discretize the RVE, A_e is the cell area and N^e the normal force vector in the cell, which is considered constant over the cell.

After imposing the macroscopic strain tensor ε to the RVE boundary, the microscopic equilibrium problem consists of finding the displacement fluctuation field $\tilde{u}_\mu^{i+1} = \tilde{u}_\mu^i + \delta\tilde{u}_\mu^{i+1}$ that satisfies Eq. (9), being $\delta\tilde{u}_\mu^{i+1}$ the fluctuations corrections to be imposed in iteration *i+1*. Thus, by applying the Newton-Raphson Method, $\delta\tilde{u}_\mu^{i+1}$ is computed by the following expression:

$$F^i + K^i \delta\widetilde{u}_\mu^{i+1} = 0 \tag{10}$$

where $\boldsymbol{F}$ is the traction vector and $\boldsymbol{K}$ the rigidity matrix, being defined as:

$$F^i = \int_{\Omega_\mu^h} B^T f_y\left(\boldsymbol{\varepsilon}_{n+1} + B\widetilde{u}_\mu^i\right) dV + \int_{\Omega_\mu^h} F_f^{\text{int}(i)} dV = \sum_{e=1}^{N_{cel}} B_e^T N^{e(i)} A_e + \sum_{ef=1}^{N_f} F_{ef}^{\text{int}(i)} \tag{11}$$

$$K^i = \sum_{e=1}^{N_{cel}} B_e^T D_N^e B_e A_e + \sum_{ef=1}^{N_f} K_{ef}^{(i)} \tag{12}$$

where $\boldsymbol{D_N}$ is the microscopic constitutive tangent relating forces and strains, $\boldsymbol{K_{ef}}$ and F_{ef}^{int} are the rigidity tangent matrix and internal forces vector of the cohesive contact finite element e_f, respectively. Also, N_f is the number of the cohesive contact finite element and B_e the cell strain-displacement matrix.

The RVE formulation is completed with the choice of kinematical constraints to be imposed on the RVE that leads to different classes of multi-scale models and therefore, to different numerical results. Three different boundary conditions can be imposed to the RVE in terms of displacement fluctuations: (i) linear boundary displacements, (ii) periodic fluctuations and (iii) uniform tractions (see more details in Souza Neto and Feijóo [9]; Fernandes, Pituba and de Souza Neto ([10], [11])). According to the formulation developed in [9], after the RVE equilibrium equation (9) is satisfied, the RVE constitutive response can be obtained. The homogenized stress tensor is computed considering the boundary tractions while the homogenized constitutive tensor is obtained considering the constitutive tensors of the cells as well as the rigidity matrix *K* (see more details in Fernandes and Pituba [12]).

6 Contact Cohesive Finite Element

In Pituba, Fernandes and de Souza Neto [8], a cohesive fracture law has been proposed in order to deal with damage process leading to the complete failure of microstructures in ductile media. Moreover, in Santos, Fernandes and Pituba [14] additional applications for the model proposed in [8] have been discussed. In general way, this model has been developed to represent the cracking process where traction is still possible to be transmitted between fracture lips. It is possible to assume the existence of a free energy potential ϕ from where the relationships of the model are derived. Besides, the deformation due to sliding opening process is assumed as a scalar value independent of the direction of sliding on the cohesive surface, thus $\delta s = |\delta s|$, therefore the behavior has an isotropic characteristic and the cohesive law is written introducing an effective opening displacement expressed by:

$$\delta = \sqrt{\beta^2 \delta_S^2 + \delta_n^2} \tag{13}$$

where, δ_n is the normal opening displacement due to mode *I*; δ_s is the sliding opening displacement due to mode *II*. The parameter β assumes different values (from *0* to *1*) to the sliding and normal opening displacements given a weight ratio between the sliding and normal directions. On the other hand, the cohesive law is expressed as:

$$\mathbf{t} = \frac{t}{\delta}(\beta^2 \boldsymbol{\delta}_\mathbf{S} + \delta_n \mathbf{n}) \tag{14}$$

where, $\boldsymbol{n}$ is the unit normal to the cohesive surface; $\boldsymbol{t}$ is the cohesive traction on the crack; *t* is a scalar effective traction. The released cohesive energy in the microstructure of the material is given by:

$$\Phi = e\sigma_C\delta_C\left[1 - e^{\left[-\left(1+\frac{\delta}{\delta_C}\right)\right]}\right] \tag{15}$$

The laws for the scalar effective traction for the loading and unloading cases are given by:

$$t = \frac{\partial\phi}{\partial\delta} = \sigma_c e^{-\delta/\delta_c} \qquad if\ \ \delta = \delta_{\max}\ \ and\ \ \dot{\delta} \geq 0 \tag{16}$$

$$t = \frac{t_{\max}}{\delta_{\max}}\delta \qquad if\ \ \delta < \delta_{\max}\ \ or\ \ \dot{\delta} < 0 \tag{17}$$

where e is the e-number, σ_c is the maximum tension cohesive normal traction and δ_c is a characteristic opening displacement that indicates a critical opening.

Before the nucleation process, it is assumed the existence of stiffness between the lips of the future fracture. This stiffness is simulated by another parameter of the proposed model called penalty factor (λ_p). In a practical point of view, high values for this parameter are adopted in order to obtain an accurate approach. This procedure ensures that the future fracture be kept closed until the separation criterion is reached and, at the same time, guarantees the physical admissibility of the entire process. The penalty factor is, therefore, a stiffness imposed to the closuring of the crack.

In general way, that strategy intends to create stiffness between the nodes of the embedded cohesive contact finite elements in the matrix zone in order not to allow penetration of the surfaces of the fracture. On the other hand, in tension regimes, this penalty factor effectively replaces the initial rigid part of the cohesive law for a linear response. In order to detect the cohesive contact phenomenon, the concept of the opening displacement gap between the Gauss points of the cohesive contact finite element is adopted.

$$t = \lambda_p\delta \qquad if\ \ \lambda_P\delta \leq \sigma_c \tag{18}$$

The finite elements used in this work are perfectly superposed to the interface elements (from the BEM model) in the undeformed configuration of the RVE. In order to represent the debonding phase, the interface nodes related to the BEM model had to be duplicated, being one collocation point adopted at the matrix and the other one inside the inclusion, separated by a very small distance. Moreover, the cohesive contact finite element is defined as an element with four nodes and its geometry is compatible with the triangle cells used to model the matrix and inclusion zones. For the formulation details about the cohesive contact finite element, see Pituba, Fernandes and de Souza Neto [8].

7 Numerical Application

In order to evaluate the BEM approach to deal with the phase debonding problem, a RVE representing the microstructure of a ductile material reinforced by a rigid inclusion is analyzed. Two situations are considered for the inclusion: perfectly bonded and phase debonding. For that, the RVE has been discretized by 580 triangular cells and 323 nodes for perfectly bonded case. When the phase debonding is considered, the same number of cells has been adopted, but 339 nodes are necessary (because the interfaces nodes are duplicated) and 16 contact cohesive finite elements, see Fig. 2. For the matrix, the following material properties are adopted: Poisson's ratio $\nu=0,3;$ Young's modulus $E=200GPa$, yield stress $\sigma_y=70MPa$ where a plastic Von Mises model with isotropic hardening $K=6.17GPa$ has been assumed. For the elastic inclusions we have adopted: $\nu=0,25$ and $E=1100GPa.$

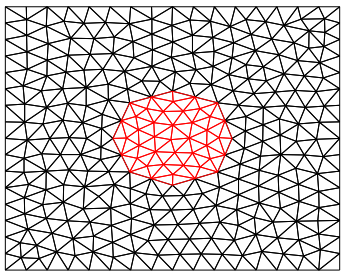

Figure 2- Discretization of the RVEs.

In all analyses, the periodic fluctuations are adopted. Besides, for the contact cohesive finite element, the following parameters are adopted (see Santos, Fernandes and Pituba [14]) : $\lambda_p = 2x10^{12}$ N/mm^3, $\sigma_c = 24$ MPa, $\beta = 0.707$ and $\delta_c = 0.02$ mm. Also, two different macroscopic strains are imposed into 35 increments to the RVEs in order to compare the proposed BEM approach to FEM approach proposed in Pituba, Fernandes and de Souza Neto [8]: $\boldsymbol{\varepsilon} = \{\varepsilon_x; \varepsilon_y; \gamma_{xy}\} = \{0.00455; -0.00455; 0\}$ and $\boldsymbol{\varepsilon} = \{\varepsilon_x; \varepsilon_y; \gamma_{xy}\} = \{0; 0; 0.00455\}$.

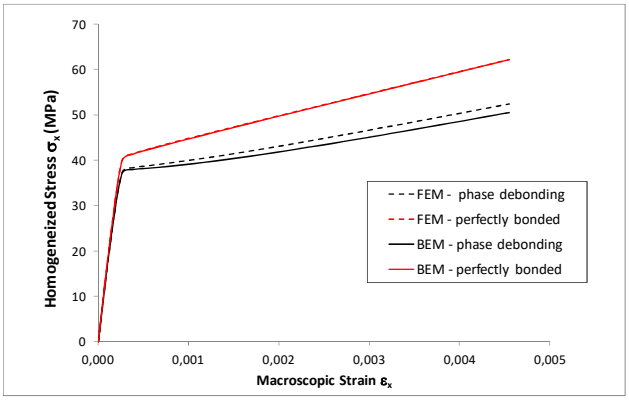

Figure 3- Homogenized stress σ_x versus macroscopic strain ε_x for the imposed macroscopic strain $\{0.00455; -0.00455; 0\}$.

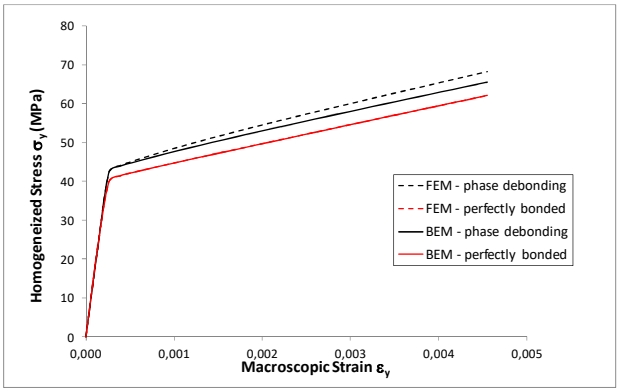

Figure 4- Homogenized stress σ_y versus macroscopic strain ε_y for the imposed macroscopic strain $\{0.00455; -0.00455; 0\}$.

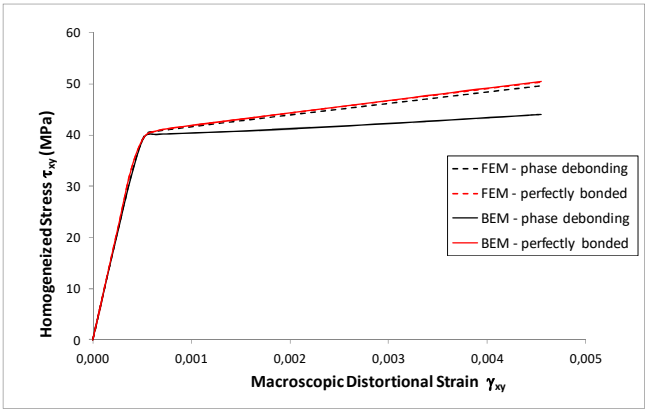

Figure 5- Homogenized stress τ_{xy} versus macroscopic distortional strain γ_{xy} for the imposed macroscopic strain *{0; 0; 0.00455}*.

In Figs. 3, 4 and 5 are presented the homogenized stress responses for the each case analyzed. For the visualization proposes, Fig. 4 presents absolute values. As can be observed, the results are very similar when perfectly bonded is considered. It is important to note in Fig. 4 that the consideration of the possible fracture process in the interface zone leads to an increasing of the strength in the y-direction due to the contact phenomena captured by the contact cohesive finite elements between the matrix and inclusion. Each Gauss point of this element contributes to the internal force evaluation by means of the traction vector computed either by the cohesive law (if a crack is opened at that Gauss point) or by the contact law (if a crack is closed at that Gauss point). Therefore, this finite element leads to crack surfaces not properly parallel. On the other hand, the BEM approach is capable to deal with large yielding process as showed in Fig. 5, where only distortional strain is imposed. In general way, considering the phase debonding, the BEM approach leads to smoother numerical responses than the FEM approach, mainly when only distortional strain is imposed.

8 Conclusions

A BEM formulation to analyze micro-structures of heterogeneous materials considering the phase debonding problem has been presented, where the RVE (Representative Volume Element) is modeled as a zoned plate. To consider the phase debonding, additional finite elements have been defined along the interfaces between the matrix and the inclusions, where a contact and cohesive fracture model have been considered. On the other hand, the inclusions have been adopted to have an elastic behavior while the material behavior in the triangle cells, defined inside the matrix domain, has been governed by the von Mises criterion. A set of examples has been presented the accuracy of the proposed BEM approach when compared to the FEM modeling.

Acknowledgements

The authors wish to thank FAPEG (Fundação de Apoio à Pesquisa do Estado de Goiás) and CNPq (Conselho Nacional de Desenvolvimento Científico e Tecnológico).

References

[1] Aliabadi MH. The Boundary Element Method: applications in solids and structures, v.2, Wiley, 577pp., 2002.
[2] Beskos D.E., *Boundary element analysis of plates and shells*. Springer Verlag, Berlin, 1991.
[3] Brebbia CA, Telles JCF, Wrobel LC. *Boundary element techniques. Theory and applications in engineering,* Springer-Verlag, Berlin and New York, 1984.

[4] Fernandes GR and de Souza Neto EA. Self-consistent linearization of non-linear BEM formulations with quadratic convergence. *Computational Mechanics.*, v.52, p.1125-1139, 2013.
[5] Fernandes G. R., Rosa Neto J. Analysis of stiffened plates composed by different materials by the boundary element method. *Structural Engineering and Mechanics, an International Journal.* v.56 No.4 p.605-623, 2015.
[6] Gal, E. and Kryvoruk, R, Fiber reinforced concrete properties – a multiscale approach, *Computers and Concrete, an International Journal*, v. 8 (5), 525-539, 2011.
[7] Nguyen, V.P. , Lloberas Valls, O., Stroeven, M. and Sluys, L.J., Homogenization-based multiscale crack modelling: from micro-diffusive damage to macro-cracks, *Comput. Methods Appl. Mech. Engrg.*, 200 (9–12), p.1220–1236, 2011.
[8] Pituba J. J. C., Fernandes G. R. & de Souza Neto E. A. Modelling of cohesive fracture and plasticity processes in composite microstructures. *Journal of Engineering Mechanics.* v. 142 (10), p. 04016069-1 – 04016069-15, 2016.
[9] de Souza Neto, E.A. & Feijóo, R.A. Variational foundations of multi-scale constitutive models of solid: Small and large strain kinematical formulation. National Laboratory for Scientific Computing (LNCC/MCT), Brazil, Internal Research & Development Report No. 16, 2006.
[10] Fernandes G. R., Pituba J. J. C. & de Souza Neto E. A. Multi-Scale Modelling For Bending Analysis of Heteregeneous Plates by Coupling BEM AND FEM. *Engineering Analysis with Boundary Elements.* v. 51 p. 1-13, 2015.
[11] Fernandes G. R., Pituba J. J. C. & de Souza Neto E. A. FEM/BEM formulation for multi-scale analysis of stretched plates. *Engineering Analysis with Boundary Elements*. V. 54, p.47-59, 2015.
[12] Fernandes G. R., Silva M. J. M., Vieira, J. F.Pituba J. J. C. A 2D RVE formulation by the Boundary Element Method Considering Phase Debonding. *Engineering Analysis with Boundary Elements.* V. 104 259-276, 2019.
[13] Fernandes G. R., Crozariol L. H. R., Furtado A. S. and Santos M. C. A 2D Boundary Element Formulation to Model the Constitutive Behaviour of Heterogeneous Microstructures Considering Dissipative Phenomena. *Eng Anal Bound Elem,* 99, p. 1-22, 2019.
[14] Santos, W. F, Fernandes G. R. and Pituba J. J. C. A. Analysis of the influence of plasticity and fracture processes on the mechanical behavior of Metal Matrix Composites microstructures. *Revista Matéria*. V. 21, p.577-598, 2016.